Impurity behaviours in ITER plasmas with standard type I ELMy *H*-mode before and after heating phase

C. Chuchinda[1], T. Onjun[1], R. Picha[2], P. Klaywittaphat[3], N. Poolyarat[4] and S. Suwanna[1]

[1]*School of Manufacturing Systems and Mechanical Engineering, Sirindhorn International Institute of Technology, Thammasat University, Klongluang, Pathumthaini, Thailand*

[2]*Thailand Institute of Nuclear Technology, Bangkok, Thailand*

[3]*Physics Department, Faculty of Science, Thaksin University, Songkhla, Thailand*

[4]*Department of Physics, Thammasat University, Pathumthani, Thailand*

Introduction

In fusion energy operation, the presence of impurities is inevitable. It contributes to radiation losses and fuel dilution, which result in a degradation of fusion performance. Helium is the most obvious and abundant impurity in fusion plasma because it comes directly from the D-T nuclear fusion reaction. Beryllium (Be) and carbon (C) are released from plasma facing components. Beryllium has been found to be able to suppress the physical and chemical erosion of carbon. Therefore, it is used as a coating layer on graphite wall [1], which will be used as a coating material in ITER. Carbon is used in strike zones of the divertor target because of its thermo-mechanical properties [2]. Furthermore, neon (Ne) is used as an extrinsic impurity. The work of Beurskens *et al*. [3] showed that an appropriate injection of Ne can reduce the ELM energy loss to be below 3% and limit ELM penetration to $r/a > 0.7$. Moreover, neon can reduce the thermal load on the divertor by radiating the power onto the main chamber [4]. The accumulation of these impurities can cause many problems such as core radiation enhancement, fuel dilution or even plasma disruptions [5]. The central heating is proven to be one method of reducing the central impurity accumulation by increasing the impurity anomalous diffusion and reducing the impurity neoclassical inward convection [6]. The recent work by Leekhaphan *et al*. [7], it was discovered that the impurity accumulation in ITER standard type I ELMy *H*-mode depends sensitively on boundary conditions and transport. Related to this matter, the boundary model based on the "dynamic boundary density model" is proposed in Ref.[8] in which the boundary conditions take the following forms:

$$n_{hyd,ped} = c_{hyd} \cdot \bar{n}_{hyd} \tag{1}$$

$$n_{imp,ped} = c_{imp} \cdot \bar{n}_{imp} \tag{2}$$

where $\bar{n}_{hyd}$ and $\bar{n}_{imp}$ are hydrogenic and impurity line-averaged density, respectively. The constants c_{hyd} and c_{imp} are respectively the hydrogenic and impurity density constants. In Ref. [9], the values of c_{hyd} and c_{imp} are found using a comparison with experimental data. It is found that the best c_{hyd} and c_{imp} are 0.77 and 0.74, respectively. With these boundary conditions combined with a core transport model, the time evolution of plasma profiles can be predicted via BALDUR integrated modelling code. In this work, we have chosen the theory-based Multimode (MMM95) model for anomalous transport calculation and NCLASS for neoclassical transport calculation of core transport.

Simulation Results

In this work, the impurity behaviours before and after turning off auxiliary power (P_{aux}) have been investigated. ITER plasma with standard type I ELMy *H*-mode is chosen for determining those behaviours. The physical parameters for this scenario are R = 6.2 m, a = 2.0 m, I_p = 15 MA, B_T = 5.3 T, $\varkappa_{95}$ = 1.70, δ_{95} = 0.33 and $\bar{n}_l$ =1.0x10^{20} m^{-3}. The total auxiliary power is 40 MW (33 MW of NBI and 7 MW of RF heating power). The plasma density is slowly ramped up during the first 100 seconds to reach the target value. During the start-up phase, the plasma current is set to be 3 MA and slowly increased to 15 MA in 100 seconds. Furthermore, the pedestal temperature (T_{ped}) in all simulations is assumed to be 3.0 keV. From all simulations, it is found that the total amount of impurity in the plasma core increases rapidly in the first 100 seconds and reaches a steady-state value. The auxiliary power is turned off at 800 s and the impurity behaviours are observed during the presence and absence of the auxiliary power.

The evolution of plasmas with different choices of impurity can be seen in Figure 1. It can be seen that when the auxiliary heating is turned off, central ion temperature and alpha power decrease. On the other hand, helium densities increase while the other impurity density used (either Be, C, or Ne) remains almost constant. Figure 2 shows the profiles of two impurity densities and the impurity diffusion coefficient for simulations with -the Multimode transport model. It can be seen that after P_{aux} is turned off, all impurity densities decrease by approximately 20.8%. For helium density, it is observed that the density increases by about 19.2%. For the impurity diffusion coefficients, the simulations with Be-He impurities and C-He impurities yield the decreasing diffusion at the region 40% of minor radius and the pedestal region. For rest of the regions, diffusions increase. For Ne-He simulation, the diffusion decreases at the regions about 25% of minor radius and the pedestal region. For rest of the regions, the diffusions increase.

Furthermore, the variation of pedestal temperature has been investigated. The evolutions of plasmas of both pedestal temperature of 2.0 and 4.0 keV are shown in Figure 3. For the pedestal temperature of 2.0 keV (Figure 4), it is observed that the impurities tend to decrease after turning off P_{aux} while He tends to increase. For the pedestal temperature of 4.0 keV (Figure 5) all impurities including He tend to increase after turning off P_{aux}.

Conclusion

From the study of the effects of P_{aux} on the impurity behaviours, we make the following conclusion. After the auxiliary power is turned off, the impurities tend to decrease while the He density tends to increase and the impurity particle diffusion coefficient tends to increase in most regions.

Acknowledgements

This work is supported by the Commission on Higher Education (CHE) and the Thailand Research Fund (TRF) under Contract No RMU5180017.

References

[1] R.P. Doerner et al., Phys. Scr. T111, 75 (2004)
[2] K. Ohya, Phys. Scr. T124, 70 (2006)
[3] M.N.A. Beurskens et al., Nucl. Fusion 48, 095004 (2008)
[4] P. Belo et al. Plasma Phys. Control. Fusion 50, 085003 (2008)
[5] Z. Yong-Zhen et al., Chin. Phys. B 18, 5406 (2009)
[6] R.Dux et al., J. Nucl. Mater. 313, 1150 (2003)
[7] P. Leekhaphan et al., to appear in TIJSAT
[8] Y. Pianroj et al., to appear in Plasma Phys. Rep.
[9] A. Siriwitpreecha et al., Proceedings of 37th EPS

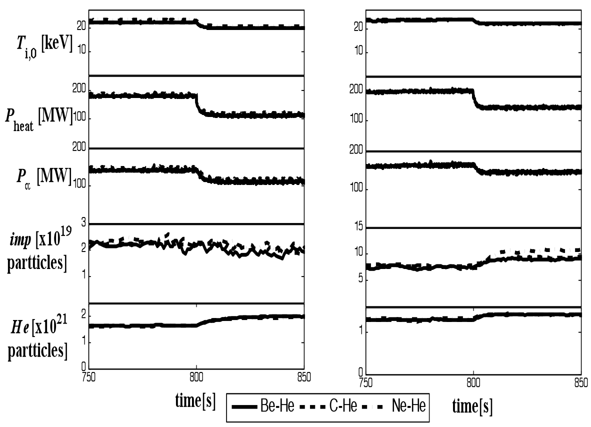

Figure 1: Time evolutions of central ion temperature, heating power, alpha heating power, total amount of impurities and helium with pedestal temperature of 3.0 keV from 750 to 850 sec. All simulations are carried out using Multimode transport model.

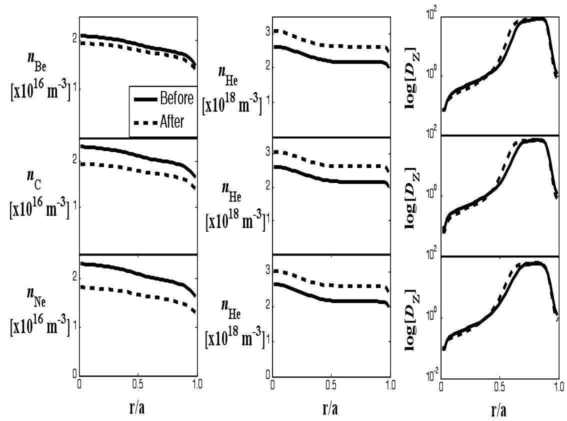

Figure 2: Profiles of impurity densities and impurity diffusion coefficients as functions of normalized minor radius for simulations Be-He (top row), C-He (middle row) and Ne-He (bottom row) with pedestal temperature of 3.0 keV. All simulations are carried out using theory-based Multimode transport model.

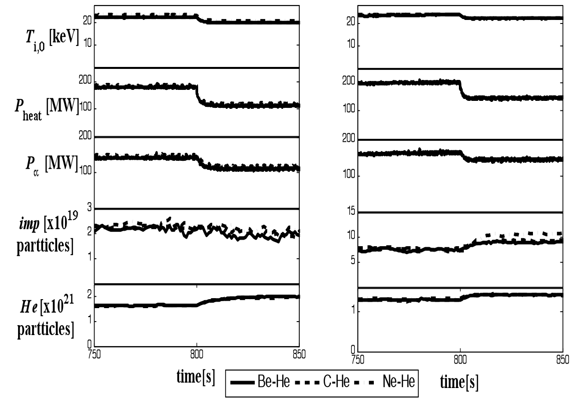

Figure 3: Time evolutions of central ion temperature, heating power, alpha heating power, total amount of impurities and helium with the pedestal temperature of 2.0 (left panel) and 4.0 (right panel) keV from 750 to 850 sec. All simulations are carried out using Multimode transport model.

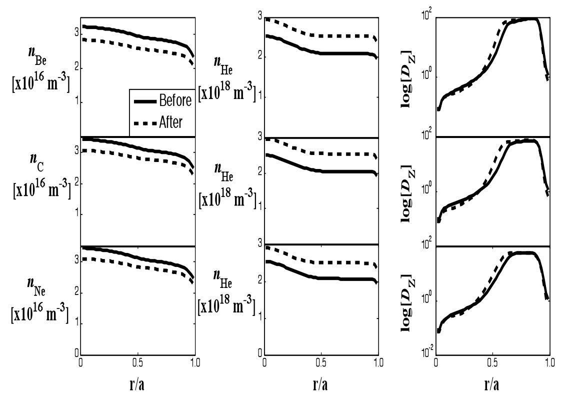

Figure 4: Profiles of impurity densities and impurity diffusion coefficients as functions of normalized minor radius for simulations Be-He (top row), C-He (middle row) and Ne-He (bottom row) with pedestal temperature of 2.0 keV. All simulations are carried out using theory-based Multimode transport model.

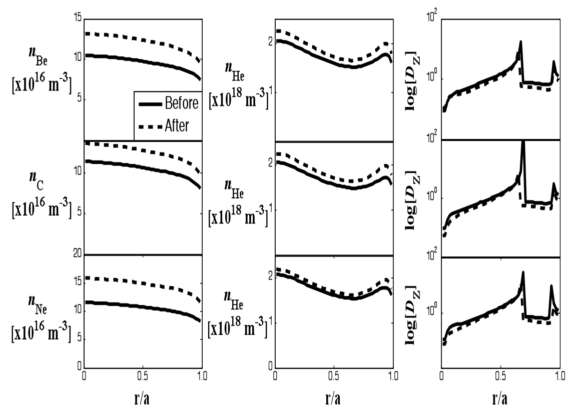

Figure 5: Profiles of impurity densities and impurity diffusion coefficients as functions of normalized minor radius for simulations Be-He (top row), C-He (middle row) and Ne-He (bottom row) with pedestal temperature of 4.0 keV. All simulations are carried out using theory-based Multimode transport model.